CHEMICAL CHANGES AND TENSILE AND ELECTRICAL PROPERTIES OF EPOXY RESIN CARBON BLACK NANOCOMPOSITES

O. Mamat and R. M. Joshua[*]

Mechanical Engineering Departmental Universiti Teknologi PETRONAS Tronoh, Malaysia

ABSTRACT

The properties of epoxy rsesin can be improved by the use of nanofiller such as carbon black (CB), The nanocomposite was synthesized by dispersion via sonication and shear mixing. The morphology, surface chemistry and the structure of CB and the epoxy/CB nanocomposites were investigated using XPS, FTIR, FESEM, and XRD. The FTIR spectrum indicates nucleophilic addition in the presence of CB nanoparticles forming hydroxyl functional group. The XRD pattern shows a slight shift in the morphology between the neat epoxy and the epoxy/CB nanocomposites. The percolation threshold is at 20 – 24 wt% loading. The resistivity of the nanocomposite decreases with CB loading from 90 Ωcm to 0.3 Ωcm at 25 wt% of CB.   The Tensile strength was increased by about 42 % at 2 wt%. However, at the percolation threshold (20- 25 wt% CB) the tensile strength was very poor at 1-2 MPa.

Keywords: Carbon Black; Epoxy Resin; Resistivity; Nanocomposite; Tensile Strength.

Epoxy resin is a broad class of versatile reactive compound, containing epoxide group, Epoxide functionality is stable under ambient conditions and is responsible for an extended shelf life.

Epoxide is an organic compound whose molecule contains a three-membered oxirane ring, compriced of an oxygen atom and two carbon atoms, these rings, however, can react with other chemical species. Epoxy is two system chemical specie and consisting of resin and curing agent. A vast choice of curing agent gives varied curing conditions such as ambient temperature, elevated temperature or by exposure to light leading to tough yield and void free networks. This backbone and cure chemistry can be manipulated to provide specific resin processing and network properties. For instance, Babayan and Calif [1] developed an improved curing agent for epoxy resin. This curing agent increases the curing temperature and provides an improved product with better properties while avoiding under curing or shortening gel time. This flexibility in the resin system provides a means to tailor resin and network properties leading to a wide area of fundamental research and commercial applications.

Epoxy chemistry was first reported by Wurtz in 1859 [2]. Manipulating the backbone chemistry on which the oxirane rings are attached is important as they result in varied product from low viscosity liquids to tack free solids, and hence result in a wide range of uses of epoxy [3] such as electromagnetic [4], structural [5], electrical, Automobile and aerospace applications [6]. The service properties of epoxy can be improved by the use of nanofiller such as silica, copper powder, graphite, carbon black (CB) etc. The propensity to realize an improved properties of the nanocomposites is influenced by the adaptability of both epoxy material and the nanofiller used in the synthesis of the nanocomposites material [7] The chemical and physical interactions between ingredients in nanocomposites play an important role in the improvement of service properties such as tensile strength and electrical properties [8].

The improvement in the end properties due to the addition of nanofiller such as CB is dependent on filler quality (surface chemistry, morphology and particle size), amount of CB, the formation of micro or nano-sized aggregations within the nanocomposites [9] and the production process which affects the dispersion of the nanofiller in the polymer matrix. Cheow, et al. [10] observed that the exterior morphology of CB has a profound impact on its wettability in polymer matrix and on properties of the end products. Scierka and Forster [11] studied epoxy polymer photodegradation with respect to the chemical changes in an epoxy

system compounded with and without TiO_2. They also studied the effect of surface treatments and concentrations of the filler on the degradation of the system when exposed to UV rays. Ghasemi-Kahrizsangi, et al. [12] discovered that an optimum load concentration of 0.75 wt% of carbon black filler in an epoxy system hindered corrosion when used as organic coating with mild steel as substrate, The study of the electrochemical behaviour and anti-corrosion properties of the system showed that they form barrier which retards corrosion even when corrosion is accelerated at 65^0C. However Zhang, et al. [13] identified nucleophilic addition reaction between glycidyl end capped poly and isophorone diisocyanate molecules which are responsible for the formation of crosslinking network throughout the epoxy/CB nanocomposites system. They suggested that the solid particle loading can affect chemical reaction of the epoxy system during curing. Their research concluded that the space volume occupied by the solid particle between the functional groups resist curing reaction resulting in an incomplete curing reaction which caused crack formation within the nanocomposites.

This paper examines the chemical changes in an epoxy system filled with carbon black nanoparticle using powder x-ray diffraction (XRD), Fourier transform infra-red spectrometer (FTIR) and X-ray Photoelectron spectroscopy (XPS). Nanoparticle dispersion within the epoxy matrix was observed using field scanning electron microscope (FESEM)

2. METHODOLOGY

Epoxy was compounded based on resin and hardener components manufactured by Smooth-On Inc, the resin is EpoxAmite® 100 and the hardener or the curing agent is 102 Medium. The resin to curing agent weight ratio is 100:29 as advised by the manufacturer. The CB used is commercially available Vulcan Xc-72R manufactured by Cabot Corporation

A mass of 2.4 g representing 12.5 wt% CB was dissolved in methanol and sonicated for 15 minutes using an 800 ml digital ultrasonic bath at 42 KHz. The obtained solution was stirred using a pensonic PM-112 hand mixer at 500 rpm for 5 minutes and then sonicated for 15 minutes to achieve a well-dispersed mixture. 20 g of epoxy resin (part A) was then poured into the mixture and further sonicated for 30 minutes. In order to obtain a good dispersion, the sonicated mixture was subjected to magnetic stirring at 750 rpm and the mixture was heated to 76 °C to evaporate the methanol. 4.8 g of hardener was added and stirred using a magnetic

stirrer at 750 RPM for 10 minutes to obtain a homogeneous suspension. The above procedure was repeated for 0, 1, 2, 5, 20 and 25 wt% of CB. The produced nanocomposites blends were poured into a mold designed according to ASTM D638 to produce tensile test samples. For the conductivity test, sample of the nanocomposites blends were poured into a mold with dimensions of 50 x 50 x 5 mm and cured at ambient temperature for 24 hours. This procedure was repeated for 15, 20, 25, 26, 27, 28, 30 wt% of CB. The resistivity of nanocomposites was measured using a DT9205A digital multimeter with aluminum as electrode. The following equations were used to calculate resistivity.

$$R = \rho\frac{L}{A} \qquad (1)$$

Where L and A are length and cross-sectional area respectively of the sample and ρ is the resistivity. The conductivity is defined as:

$$C = \frac{1}{\rho} \qquad (2)$$

XPS, FESEM, FTIR and XPS were used to observe physical or chemical changes in the samples.

2.1 Field Emission Scanning Electron Microscope (FESEM)

The elemental constituent, particle size and surface morphology of CB and the produced nanocomposites were investigated using a variable Pressure Field Scanning Electron Microscope (model; Zeiss Supra55 VP) equipped with energy dispersive x-ray (EDX) microanalysis system. The system recognizes the x-rays emitted from the test pieces because of the rich-energy electron ray piercing into the test piece. The x-ray spectra was retrieved and examined, to obtain a quantitative data of the basic constituent of the test piece. The procedure has an accuracy of 1-2 % for a number of elements down to 0.1 weight percent.

2.2 Powder X-ray Diffraction (XRD)

The XRD information analysis was carried out using a Bruker AXS D8 Adance X-ray diffractometer at Universiti Teknologi PETRONAS. Powdered sample was scanned from $10\text{-}80^0$ in 2 theta scope with 0.03^0 movement interval and 2s per step response time. Origin lab- 8.0 software was used for deconvolution of the diffractogram in the 2 theta region of $18\text{-}32^0$. The nanocomposites samples were grinded to a fine powder prior to XRD analysis.

The XRD analyses were conducted for nanoparticles, neat epoxy and the epoxy/CB nanocomposites.

2.3 Fourier Transform Infra-Red Spectrometer (FTIR)

The carbon black nanoparticles, neat epoxy and epoxy/carbon black nanocomposites were analyzed using the PerkinElmer Spectrum One FTIR Spectrometer with Specac single reflection diamond ATR and Spectrum software version 5.0.1. The samples were run from 4000 cm^{-1} to 450 cm^{-1} with eight scans at a scan speed of 0.20 cm/s and a resolution of 4.00 cm^{-1}, Large sample pieces were cut using a razor blade to produce a fresh surface for analysis. Each sample was placed on the ATR diamond so that it was entirely covered and the sample was analyzed. The resulting spectrums were normalized to 1.0 and their major peaks were labeled accordingly.

2.4 X-Ray Photoelectron Spectrometer (XPS)

The samples were transferred through vacuum transfer module for moving air-sensitive samples from a glove box into the K-alpha x-ray photoelectron spectrometer made by Thermo Scientific. The samples were exposed to multiple cycles of XPS analysis and ion beam sputtering to build the final XPS depth profile. High resolution XPS spectrum were acquired with integrated monochromated dual mode ion source (1486.68 eV) in scan mode with a small spot size of 400 μm,   pass energy of 200 eV for the survey scans, and 70 eV for the elemental scans. Spectrums were then collected at each emission angles by tilting the specimens. Data analysis was performed with Avantage$^©$ software (Thermo Scientific). Generally, 10 scan integration were sufficient for obtaining elemental spectra with high signal to noise ratio.

2.5 Tensile Test

The tensile test was done in accordance to ASTM D638 using GOTECH 5 KN UTM at a crosshead speed of 5mm/min.

3. RESULTS AND DISCUSSION

3.1 FESEM

Figure 1B shows a well dispersed network of CB nanoparticle within the epoxy matrix which is distinct from the neat epoxy shown in Figure 1A. However, Figure 1C shows a highly agglomerated CB nanoparticle.
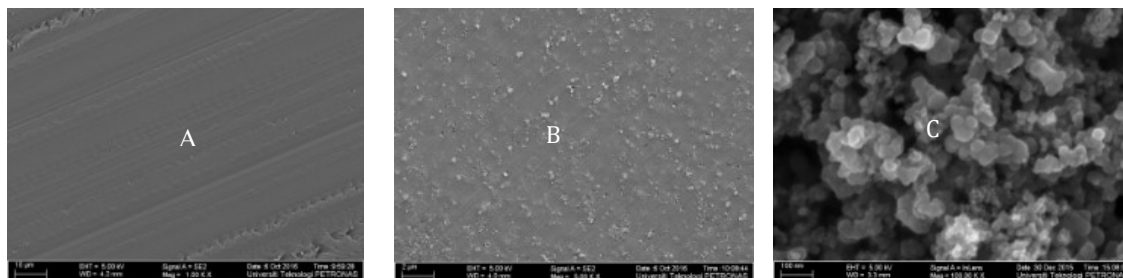

Fig.1. FESEM image of (A) neat epoxy (B) epoxy/CB nanocomposites and (C) CB nanoparticle.

3.2 Resistivity

The morphological structure of CB (Vulcan Xc-72R) is shown in the XRD image of Figure 7 with a characteristic amorphous structure. The TEM image of Figure 8 shows a porous sphere with extremely high structure while the BET analysis indicated a large surface area of 221 m^2/g. These physical properties have a profound effect on the resistivity of the nanocomposites. When mixed with epoxy resin; the hollow sphere structure can interpenetrate the epoxy chain forming chains and aggregate (Figure 1B) having a dimension in the nanometer range separated by a narrow gap. At a very low CB content, the nanocomposites are in the insulator state and, therefore, their resistivity is of a high value. Further addition of CB lowered the resistivity of the nanocomposites until a critical CB concentration was reached, where a little change in CB loading resulted in a large change in the resistivity as shown in Figure 2 and 3. This critical concentration of CB is known as percolation threshold and it is influenced by the arrangement and dispersion of CB within the epoxy resin.

Figure 3 shows the percolation threshold could be found at 20-25 wt% CB. The percolation threshold is largely affected by the shapes and sizes of the carbon aggregates and these values are affected by the degree of dispersion and morphology of the CB nanoparticles. The electrical behavior of the nanocomposites in relation to the CB loading can be categorized

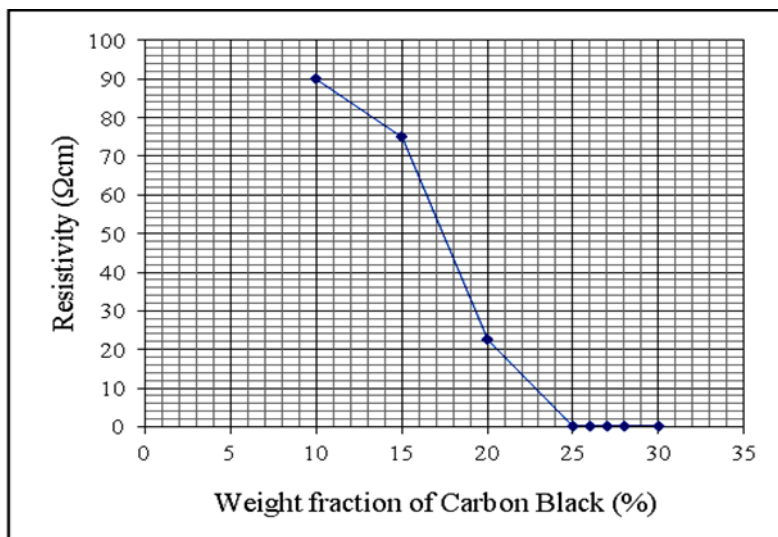into three distinct divisions: the dielectric, transition and the conducting states.

Fig.2. Resistivity of Nanocomposites with CB Filler loading.

The concept of electron tunneling in dispersed CB offers an acceptable explanation for the electrical conductivity of the nanocomposites [14]. According to this mechanism, electron may pass through thin insulating epoxy films existing between adjacent CB particles or aggregate. The existing current is an exponential function of the distance between the particles [15]. It can be inferred that the smaller the particle the wider the gap between them (Note: the CB particle diameter is 50-70 nm). At high loadings, this gap was exceedingly small probably in nanosize range and the resistance within the gaps reduced to a negligible value, resulting in conductivity. Thus a high structure as shown in Figure 8 consisting of porous structure with cavities displays a smaller distance than solid particles. This invariably lead to considerable improvement in electrical conductivity.
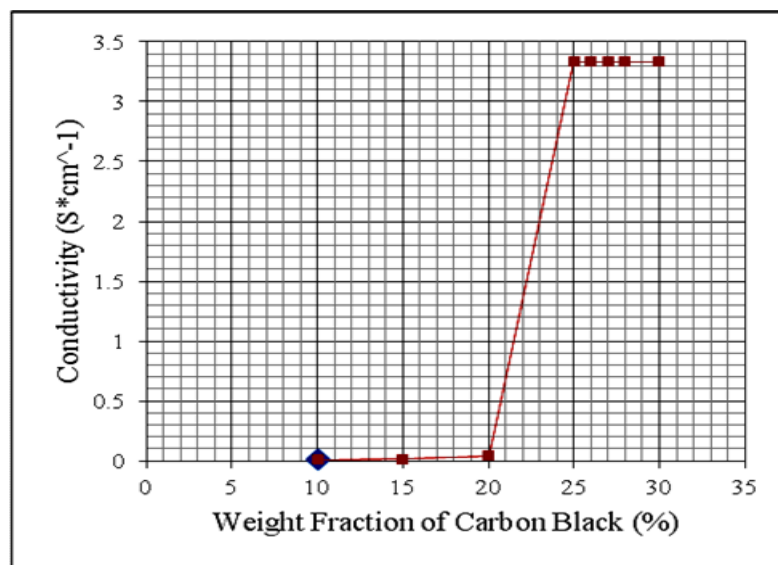
Fig.3. Conductivity of nanocomposites with CB loading

3.3 Tensile Strength

The effects of CB loading on tensile strength of epoxy resin is shown in Figure 4, at low CB loading the tensile strength of epoxy was improved with the maximum strength achieved at 2 wt% loading. Unfortunately, the tensile strength of the nanocomposites at the percolation threshold (20–25 wt%) is very low i.e. a value of between 1 -2 MPa. This means that the nanocomposites will require modifications to improve dispersion and consequently their structural property. During the polymerization reaction, the CB nanoparticles occupy a space between the functional groups of the matrix. At reasonable low filler loading there is an interfacial interaction between the matrix and the filler resulting in nanocomposites with improved tensile strength. At higher nanofiller loading there is a competition for space between the functional groups and the nanofiller, this prevent the polymerization reaction and results in an incomplete curing and consequently decreases tensile strength of the nanocomposites. The FTIR spectrum shows reduction in the number of peak for the nanocomposites. This is because the bond strain within epoxy resin makes the three membered oxirane rings susceptible to both nucleophilic and electrophilic ring opening reactions. It is worthy to note that nucleophilic addition to an asymmetric epoxide rings occurs predominantly at the least hindered site under neutral or basic conditions.
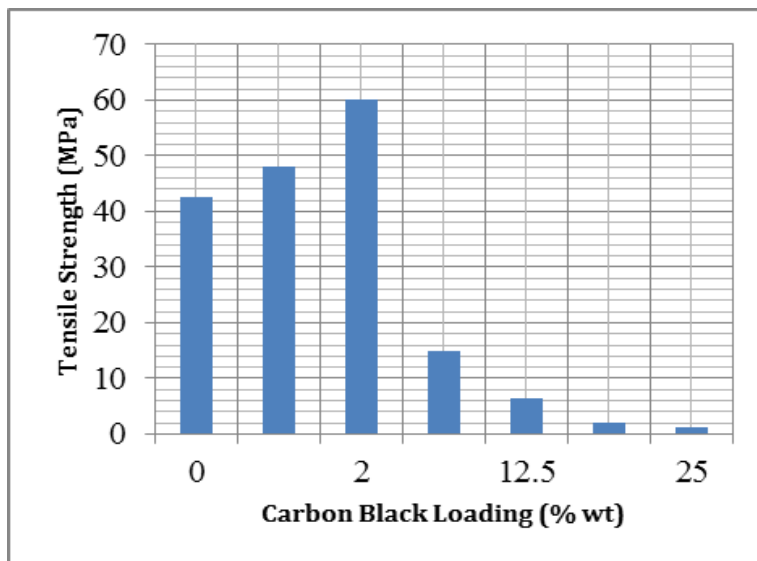
Fig.4. Effects of carbon black loading on the tensile strength of epoxy

3.4 FTIR

The steric effect which states that atoms most occupy space, forces atoms closely place to each other to have a cost in energy. When nanofiller are used in epoxy the surface chemistry of the atoms which is characterized by outer electrons will repel each other, CB as an electron donating group will append to the oxirane ring of the epoxy thus accelerating the reaction by aiding dissociation of the carbon – oxygen bond, forming nucleophile carbon bond in its place. Upon cure of epoxide with most nucleophiles polar hydroxyl groups are formed that interact favorably with hetero atoms on the surfaces of adhered substrate. The carboxylic and phenolic functional groups are shown in Figure 5, for the epoxy nanocomposites these functional groups occurred at 2921.31 and 3434.78 cm^{-1} respectively, this is an indication of nucleophilic addition.
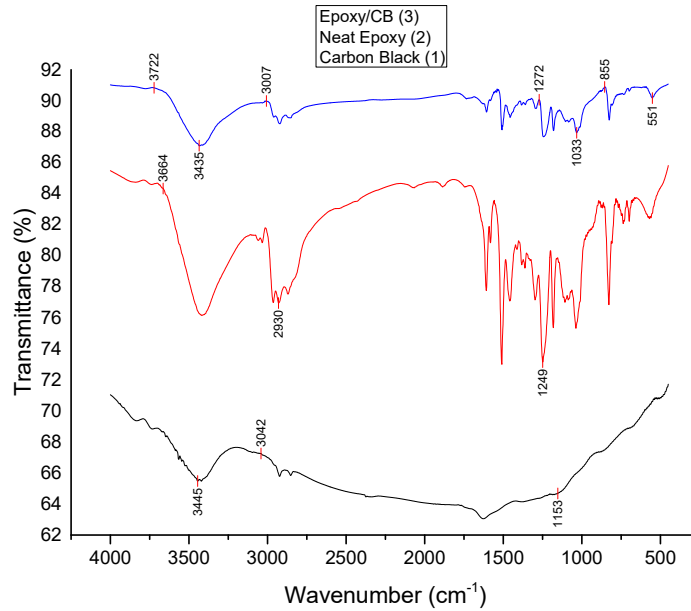
Fig.5. FTIR spectrum of CB, epoxy and nanocomposites

3.5 XPS

XPS is a powerful analytical technique to evaluate compositions of CB nanoparticle by establishing data about the surface chemistry (up to a sample depth of about 10 nm). The XPS analysis shows a spectra consisting of a C1s peak and a substantial O1s peak at 284.58 and 532.98 eV respectively. The presence of O1s peak is probably due to intrinsic surface carboxyl or phenolic groups. The XPS spectrum of Fgure 6 also shows two S2p peaks   at 163.98 and 165.18 eV. The wetting of a solid surface by a liquid and the concept of contact angle (θ) was first suggested by young [16].

$$\gamma_s + \gamma_{SL} = \gamma_L \cos\theta \qquad (3)$$

where γ_L is the surface energy of the liquid, γ_{SL} is the interfacial energy of solid/liquid interface and γ_s is the surface energy of the solid. However, Fowkes [17] further divided the surface free energy of substance into the London dispersive   and polar   components   as follows

$$\gamma = \gamma^L + \gamma^{SP} \qquad [4]$$

Where γ^L is the London dispersive component and γ^{SP} is the polar components.   For the CB nanoparticle the graphitic character influences the surface free energy as indicated by C1s
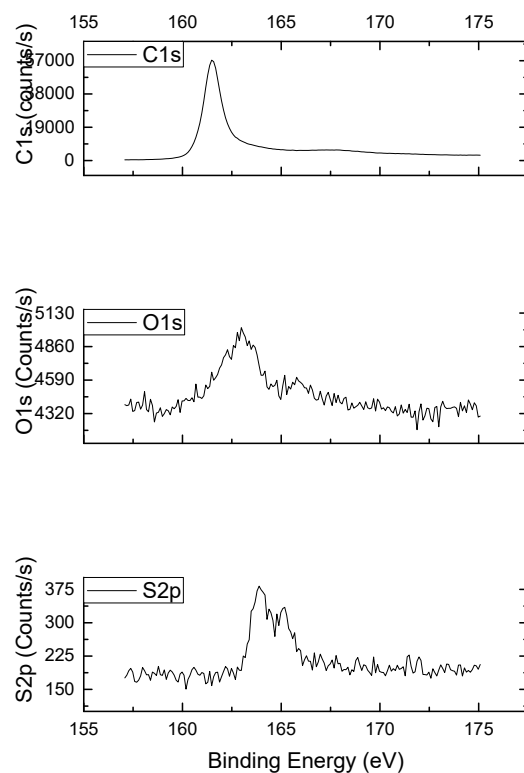
peak at 284.58 eV.

Fig.6. XPS peaks for carbon black nanocomposites

3.6 The Morphology of Nanoparticle, Neat Epoxy and Epoxy Nanocomposites

The XRD profiles of the samples are presented in Figure 7. There are two unique peaks at 22.41^0 of high intense and a somewhat broaden peak at 41.35^0. The important (002) peak at 22.41^0 is assigned to the graphitic carbon in the sample. This peak at 2θ angle of 41.35^0 can be easily assigned to (100) diffraction of graphene. The image shows the existence of both amorphous and crystal structures in the morphology of CB. The high structure as shown in the TEM image of Figure 8B explains the presence of the amorphous phase. The neat epoxy exhibited two amorphous broad peaks at 2θ = 16.75^0 and 42.77^0 and the epoxy/CB nanocomposites exhibited an intense amorphous peak at 17.17^0 and a lower broad peak at 41.80^0. The basilar reflection peak of the nanoparticle at 2θ = 22.41 is slightly shifted to 2θ = 17.17^0 for epoxy/CB nanocomposite spectrum because of the wetting of the nanoparticles with epoxy forming a well dispersed network.
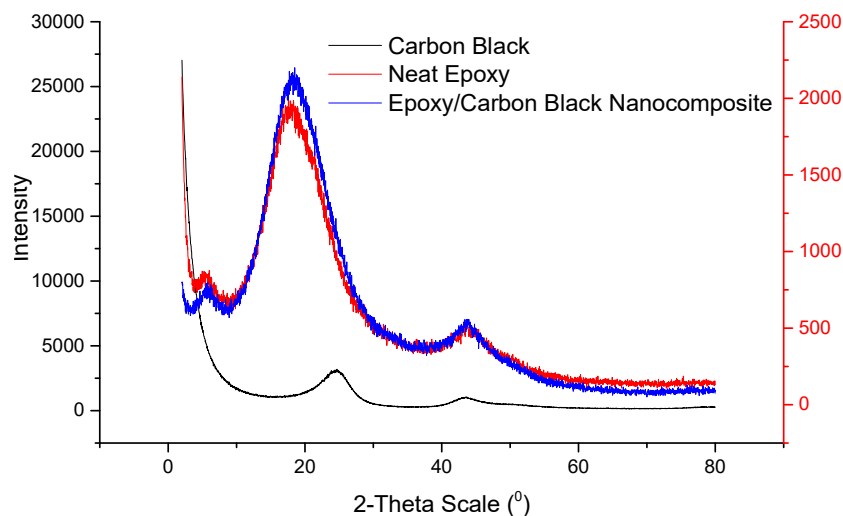
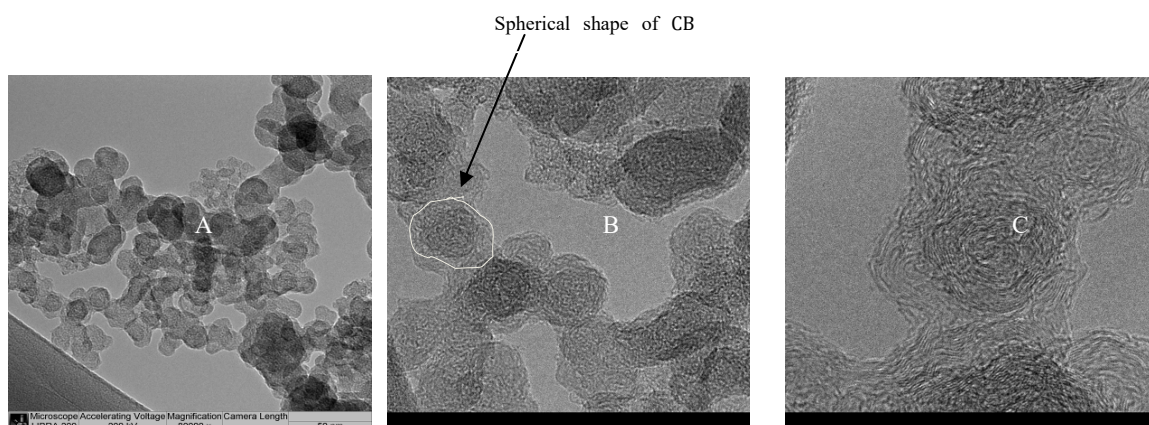**Fig.7.** XRD pattern of CB, Epoxy and the Epoxy/CB nanocomposites

Fig.8. TEM images of CB nanoparticles

4. CONCLUSIONS

XPS is a powerful tool for describing the surface chemistry of carbon black nanoparticles. FTIR was used to indicate changes in the functional groups of the epoxy as they underwent nucleophilic addition in the presence of CB nanoparticles during the curing process. The FESEM image of the nanocomposites shows a fairly dispersed but yet agglomerated particle of CB within epoxy resin. This is due to the influence of morphology and size of the CB. Similarly, the conductivity of the nanocomposites resulted from the network of CB

nanoparticles with an established percolation threshold of 20 -25 wt% CB. A high CB loading at the percolation region resulted in poor tensile strength (1-2 MPa) of the nanocomposites. The resistivity of epoxy decreased with CB loading from 90 Ωcm at 10 %wt of CB to 0.3 Ωcm at 25 wt% of CB.

5. ACKNOWLEDGMENT

6. REFERENCES

[1]　　Babayan E. P. and Calif I., Curable epoxy resin composition containing a substituted diurea compound United States Patent Application Publication, 1973.

[2]　　Ellis B., Introduction to the chemistry, synthesis, manufacture and characterization of epoxy resins, in Chemistry and Technology of Epoxy Resins, 1st edition ed: Chemistry and Technology of Epoxy Resins, 1993, pp. 1-36.

[3]　　Hamza M. S., Majeed A. H., and Kareem H. R., Enhancing Thermal and Water Absorption Properties of Unsaturated Polyester and Epoxy by Nanocarbon Black Powder, Eng. &Tech. Journal, 2013, vol. 31.

[4]　　Dorigato A., Giusti G., Bondioli F., and Pegoretti A., Electrically conductive epoxy nanocomposites containing carbonaceous fillers and in-situ generated silver nanoparticles, Express Polymer Letters, 2013, vol. 7, pp. 673-682, doi: 10.3144/expresspolymlett.2013.64.

[5]　　Khalil H. P. S. A., Jawaid M., Firoozian P., Alothman O. Y., Paridah M. T., and Zainudin E. S., Flexural Properties of Activated Carbon Filled Epoxy Nanocomposites, The Malaysian Journal of Analytical Sciences, 2014, vol.　18, pp. 391 - 397　.

[6]　　Kuzhir P., Paddubskaya A., Plyushch A., Volynets N., Maksimenko S., Macutkevic J., et al., Epoxy composites filled with high surface area-carbon fillers: Optimization of electromagnetic shielding, electrical, mechanical, and thermal properties, Journal of Applied Physics, 2013, vol. 114, p. 164304, doi: 10.1063/1.4826529.

[7]   Abdul Khalil H. P. S., Firoozian P., Bakare I. O., Akil H. M., and Noor A. M., Exploring biomass based carbon black as filler in epoxy composites: Flexural and thermal properties, Materials & Design, 2010, vol. 31, pp. 3419-3425, doi:10.1016/j.matdes.2010.01.044.

[8]   Zhang W., Dehghani-Sanij A. A., and Blackburn R. S., IR study on hydrogen bonding in epoxy resin–silica nanocomposites, Progress in Natural Science, 2008, vol. 18, pp. 801-805, doi:10.1016/j.pnsc.2008.01.024.

[9]   Marra F., D'Aloia A., Tamburrano A., Ochando I., De Bellis G., Ellis G., et al., Electromagnetic and Dynamic Mechanical Properties of Epoxy and Vinylester-Based Composites Filled with Graphene Nanoplatelets, Polymers, 2016, vol. 8, p. 272, doi:10.3390/polym8080272.

[10]   Cheow K. Y., Teh S. A. G. L., and Phua-Jin P. L., Effect of Surface Treatment on Carbon Black Filled Epoxy Composites, Journal of Applied Sciences Research, 2015, vol. April, pp. 6-12.

[11]   Scierka S. and Forster A., An XPS study on the effects of pigment on the UV degradation of an epoxy system, Proceedings of the 81st Annual Meeting Technical Program of the FSCT, 2003.

[12]   Ghasemi-Kahrizsangi A., Shariatpanahi Neshati H., J., and Akbarinezhad E., Corrosion behavior of modified nano carbon black/epoxy coating in accelerated conditions, Applied Surface Science, 2015, vol. 331, pp. 115-126, doi:10.1016/j.apsusc.2015.01.038.

[13]   Zhang W., Blackburn R. S., and Dehghani-Sanij A. A., Effect of solid particle loading on nucleophilic addition of epoxy-resin to isophorone diisocyanate, Particuology, 2008, vol. 6, pp. 24-29, doi:10.1016/j.cpart.2007.10.005.

.

[14]   Van Beek L. K. H. and Van Pul B. I. C. F., Internal Field Emission in Carbon Black - loaded natural rubber vulcanizates, Journal of Applied Polymer Science, 1962, vol. 6, pp. 348-354, doi: 10.1002/app.1962.070062408.

[15]   Verhelst W. F., K. Wolthuis G., Voet A., Ehrburger P., and D. J. B., The Role of Morphology and Structure of Carbon Black in the electrical Conductance of

Vulcanizates, Rubber Chemistry and Technology, 1977, vol. 50, pp. 735-746, doi.org/10.5254/1.3535171.

[16]   Kinloch A. J., A review of: Adhesion and Adhesives: Science and Technology. London and New York: Chapman and Hall, 1987 .

[17]   Subedi D. P., Contact Angle Measurement for The Surface Characterization of Solids, The Himalayan Physics, 2011, vol. Vol. II, pp. 1-4.